Observation of Phase Transitions of 1-Dimensional Ion Clouds in a Linear RF Trap

Mitsutoshi ARAMAKI, Satoshi KAMEYAMA, Tatsuo SHOJI, and Akihiro KONO
Nagoya University, Furo-cho, Chikusa-ku, Nagoya, 464-8603, Japan

Yoichi SAKAWA
Institute of Laser Engineering, Osaka University, Yamadaoka, Suita, Osaka, 565-0871, Japan

(Received: 19 September 2008 / Accepted: 28 October 2008)

Our goal is to study the effects of long-range correlations among ions in regard to their statistical characteristics using ion clouds confined in a linear rf ion trap. It is important to generate a simple ion cloud which shows the smooth phase change between gas and solid for detailed research on the effects of the Coulomb interaction. The competition between rf-heating and laser-cooling effects usually leads to a discrete change in ion temperature; therefore, the generation of rf-heating free ion clouds is required. In this paper, the difference in the cooling process of 3-dimensional and 1-dimensional ion clouds is discussed. The smooth phase change in 1-dimensional ion clouds is confirmed by observing the cooling process.

Keywords: strongly coupled plasma, rf trap, laser cooling, Coulomb crystal

1. Introduction

An rf ion trap (Paul trap) is a device that confines charged particles using an rf electric field. Coulomb systems composed of ions trapped in an rf trap are suitable for detailed research on long-range correlating systems, since the interaction between the trapped ions and surrounding environment is weak, and the scale of the system can be easily controlled. In addition to this, the temperature of the trapped ions can be cooled to lower than 1 K by applying laser-cooling techniques. The correlation among the trapped ions is indicated by the Coulomb coupling parameter Γ, defined as the ratio of the Coulomb interaction energy between ions to the thermal energy of ions:

$$\Gamma = Q^2 / 4\pi\varepsilon_0 a_{ws} k_B T \ .$$

Here, ε_0 is the permittivity of the vacuum, Q is the charge of an ion, k_B is the Boltzmann's constant, T is the temperature, and a_{WS} is the Wigner-Seitz radius:

$$a_{ws} = (3/4\pi n)^{1/3},$$

where n is the number density of the ions. The plasma with Γ larger than 1 is called as strongly-coupled plasma. If Γ exceeds 172, the plasma is crystallized. It is possible to generate a gas-, liquid- or solid-state ion cloud in the ion trap, since the temperature of trapped ions can be controlled over a wide range by the laser cooling techniques. The gas-state plasma is well described by Boltzmann-Gibbs (BG) statistics; however, the validity of BG statistics for the strongly correlated systems is not clear. Recently, several types of non-BG statistics which describe the long-range correlated system have been proposed. The Tsallis entropy is one of the possible generalizations of the Boltzmann-Shannon entropy, which is defined as

$$S_q[p] = \frac{k_B}{1-q}\left[\sum_{i=1}^{W} (p_i)^q - 1\right],$$

where p_i is the probability associated with an event, W is the total number of possible configurations, and q is the parameter introduced for the generalization [1]. Many pieces of theoretical and experimental research on Tsallis statistics have been reported [2]; however there is no clear explanation of how q can be determined in individual experimental systems. On the other hand, the non-extensibility of the Tsallis entropy implies the suitability for a system governed by long-range interaction.

Our goal is to study the effects of the long-range correlations among ions in regard to their statistical characteristics using ion clouds confined in a linear rf ion trap. The dynamics of the trapped ions is governed by rf heating, laser cooling (or heating), and Coulomb interaction [3]. Rf heating usually complicates the ion dynamics, therefore the generation of rf-heating free ion clouds is required. In this study, we used a linear rf trap. One of the advantages of a linear rf trap is the absence of the direct coupling between the ion motion and the rf electric field in the direction of the trap axis. The effects of rf heating in the radial direction is coupled to the axial motion via the Coulomb interaction in 3-dimensional (3D) ion clouds. Since the rf electric field is negligible on the trap axis, 1-dimensional (1D) ion clouds aligned on the

author's e-mail:aramaki@nuee.nagoya-u.ac.jp

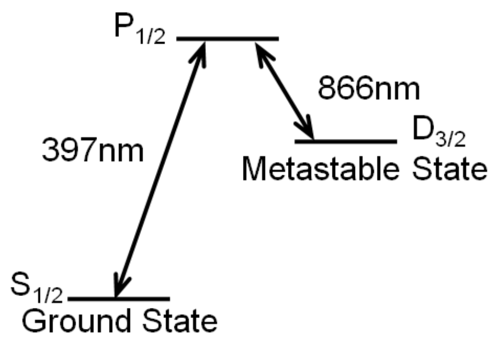

Figure 1 Diagram of the relevant states of Ca^+ laser cooling.

trap axis are the ideal Coulomb system that minimizes rf heating effect.

In this paper, the laser induced fluorescence (LIF) spectrum and the images of the 1D and 3D ion clouds were observed during the cooling process. The advantage of the 1D ion cloud is described from the viewpoint of the controllability of the ion temperature.

2. Experiment

A linear rf trap was installed in a stainless steel chamber evacuated to less than 3×10^{-10} Torr using an ion getter pump. The trap was composed of four cylindrical rf electrodes and two dc end-electrodes. The rf and dc electrodes were made of copper and stainless steel, respectively. The diagonal distance of the surface of the rf electrodes was 8.8 mm, and the diameter of the rf electrodes was 4 mm. Voltage applied to the rf electrodes was 180 ~ 210 V at 2.8 MHz. Distance between the two dc electrodes was 20 mm. Confinement of ions in the axial direction was achieved by the static field generated by the dc electrodes. Voltage applied to the dc electrode was 4 ~ 60 V.

$^{40}Ca^+$ was used in our experiment, since all the transitions of the cooling cycle can be driven by commercial laser diodes. A calcium vapor oven and an electron gun were arranged face to face on both sides of the ion trap. To decrease the calcium contamination of the trap electrodes, calcium vapor was collimated by a skimmer. The calcium vapor and the electron beam were introduced to the confinement region, and the ions were generated by electron bombardment of the calcium vapor. Generated ions were cooled using laser cooling techniques. The relevant states of $^{40}Ca^+$ laser cooling are shown in Fig. 1. Since approximately 90% of the $P_{1/2}$ state ions decayed to the $S_{1/2}$ state, the $S_{1/2}$-$P_{1/2}$ transition, excited by a 397-nm laser, was the main cooling-transition. The LIF of the 397 nm light was used to observe the cooled ions. A portion of the ions excited in the $P_{1/2}$ state fell into the meatastable $D_{3/2}$ state; therefore an 866-nm laser was used for re-pumping the ions in the $D_{3/2}$ state to the $P_{1/2}$ state. The frequency of the re-pumping laser was continuously swept around the resonance frequency to cover the Doppler broadening of the $D_{3/2}$- $P_{1/2}$ transition.

Figure 2 shows the schematics diagram of the experimental setup. The 866 and 794-nm laser lights were obtained by extended-cavity diode lasers (ECDL). The output power of the 866-nm and 794-nm ECDLs were 10

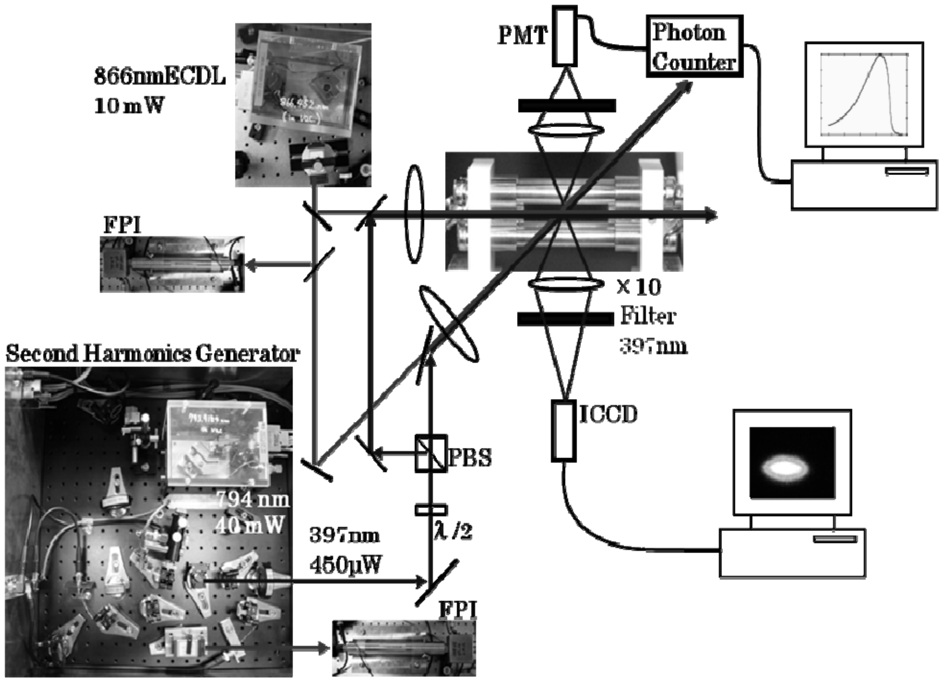

Figure 2 Schematic diagram of the experimental setup.

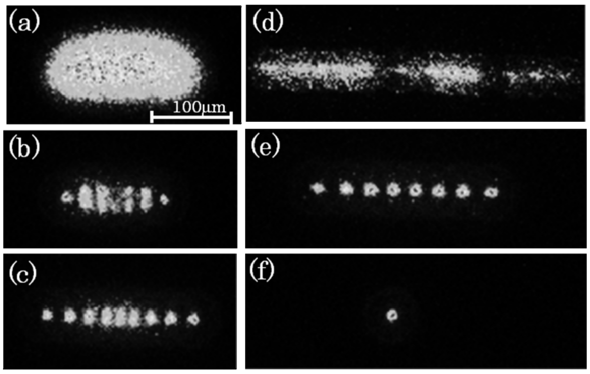

Figure 3 Generation of ellipsoidal and string ion crystal.

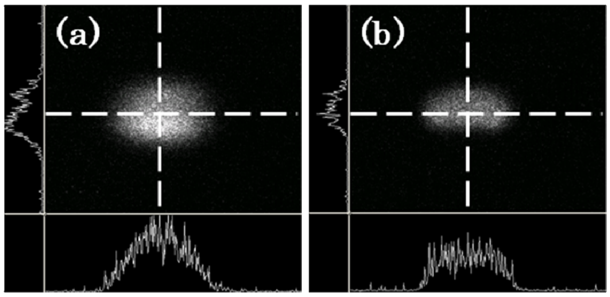

Figure 5 ICCD images of ion cloud taken at the point of “a” and “b” in Fig. 4.

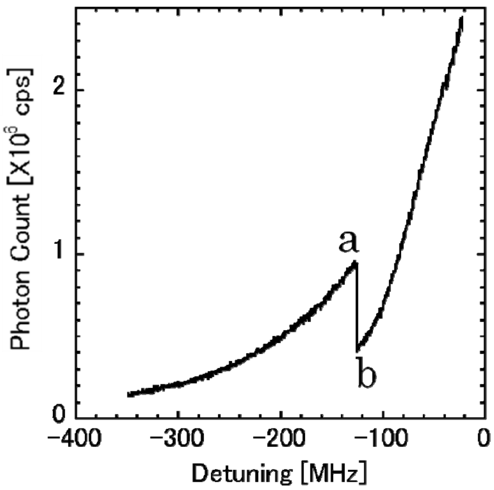

Figure 4 LIF spectrum of the 3D ion cloud (Fig. 3a).

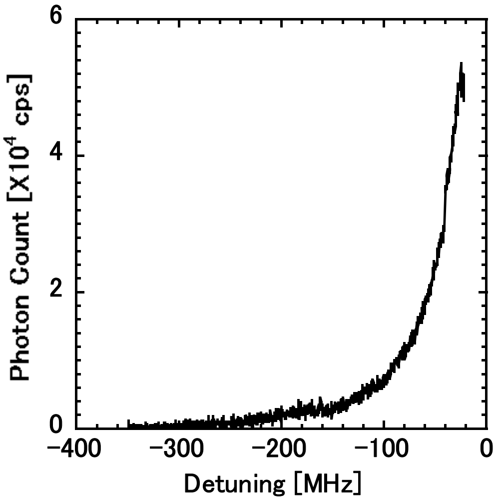

Figure 6 LIF spectrum of the 1D ion cloud (Fig. 3d).

and 40 mW, respectively. The spectra of the laser lights were monitored using Fabry-Perot interferometers (FPI) to confirm single-mode operation of the ECDLs. The 397 nm laser light was obtained by the second-harmonic generation (SHG) of the 794-nm laser light using a nonlinear crystal (LBO) installed in a ring cavity. The power of SHG was 450 μW. Since the temperature of laser-cooled ions is sensitive to the frequency of the 397-nm laser, the short-term fluctuation and the long-term drift of the laser frequency was stabilized by using optical feedback from the ring cavity and controlling the resonator length of the ring cavity respectively [4, 5]. The 397 and 866-nm lasers were divided into two components and superimposed before being introduced from 0° and 45° to the trap axis. Two degrees of freedom of ions were cooled simultaneously. The LIF signal of the $S_{1/2}$-$P_{1/2}$ transition was used for ion detection. The ion cloud was observed from the side of the linear trap. Integration of the LIF signal was detected using a photomultiplier tube (PMT) and a photon counter. The image of the ion cloud was observed using an intensified charged coupled device (ICCD) camera with a 10-magnification imaging-lens system.

3. Results

Figure 3 shows the images of the ion clouds confined in the linear rf trap. The cloudy state ions (Fig. 3a) were crystallized by decreasing the number of ions (Fig. 3b). The number of trapped ions was decreased by shutting down the re-pumping laser and decreasing the confinement potential. 1D ion crystal was made of the ellipsoidal ion crystal by changing the ratio of the radial-to-axial confinement potentials (Fig. 3d). The ion clouds in the left column (Fig. 3a-c) are classified as 3D ion clouds; on the other hand, the ion clouds in the right column (Fig. 3d-f) are classified as 1D ion clouds. The cooling processes of the 3D ion cloud (Fig. 3a) and the 1D ion cloud (Fig. 3d) were observed.

Figure 4 shows the LIF spectrum of the middle-sized 3D ion cloud (Fig. 3a). Here, the rf voltage and dc voltage were 180 V and 60 V respectively. Since the laser cooling technique works by tuning the frequency of the cooling laser below the cooling transition, the LIF spectrum was obtained by sweeping the frequency of the 397-nm laser from the low frequency side to the resonance center

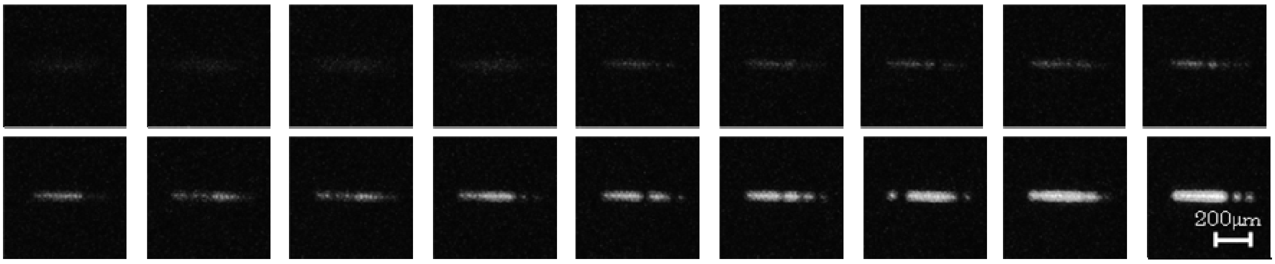

Figure 7 Sequential images taken during the cooling process of the 1D ion cloud (Fig. 3d). The cooling process is depicted beginning from the image in the upper-left and ending with the final image in the lower-right.

(755.4361 THz). The horizontal axis of the spectrum is the frequency of laser tuning. The LIF spectrum showed a discrete drop at -130 MHz. The ion temperature was roughly estimated as 3 K using the LIF spectrum of the range of -130 to -20 MHz. The mechanism of the sudden drop is not fully clarified yet; however it is thought that the changes in the relation between rf heating and the laser cooling effects causes the discrete change [6]. Figures 5(a) and 5(b) show the images taken at the point “a” and “b” in Fig. 4, respectively. Intensity distributions at the cross sections indicated by the broken lines are also displayed. Simultaneously with the change of the LIF spectrum, the radial distribution of the ion cloud shrank, and the ion distribution in the axial direction changed from a hump type to a plateau type. The change of the intensity distribution indicated a sudden drop of the ion temperature and a rapid growing of the effect of the Coulomb interaction among ions. Since we plan to study the effects of the Coulomb interaction by sweeping the ion temperature, the discrete change of the ion temperature is inconvenient. Figure 6 shows the LIF signal of the 1D ion cloud (Fig. 3d). Here, the rf voltage and dc voltage were 210 V and 4 V, respectively. The LIF spectrum did not show a clear fluorescence dip, since the ions were confined on the trap axis where the rf heating effect was negligible. Sequential images taken through the cooling process of the 1D ion cloud showed a smooth phase change from gas to solid (Fig. 7). The smooth controllability of this phase of the ion cloud was a great advantage for the study of the effect the Coulomb interaction.

4. Conclusion

The cooling process of the 3D and 1D ion clouds was studied to find out a suitable ion cloud for the research of the effects of long-range correlations among ions on their statistical characteristics. The LIF spectrum and the images of the 3D ion cloud showed the existence of discrete changes in ion temperature during the cooling process. Since a detailed study in the vicinity of the border between weakly- and strongly-coupled plasmas is important, the discrete changes in ion temperature are inconvenient. On the other hand, the state of the 1D ion cloud smoothly changed from the cloudy state to the solid state, because rf heating was negligible for the 1D ion cloud confined on the trap axis. The experimental results showed the advantage of the 1D ion cloud to study the effects of the Coulomb interaction on the characteristics of ion clouds.

5. Acknowledgements

The authors would like to thank Dr. K. Hayasaka for his valuable advice and discussions. This work was partially supported by the Ministry of Education, Science, Sports and Culture, Grant-in-Aid for Scientific Research (C).

[1] C. Tsallis, *J. Stat. Phys.* **52**, 479 (1988).
[2] For a regularly updated bibliography see http://tsallis.cat.cbpf.br//biblio.htm
[3] Y. Maeno, M. Tachikawa, Y. Moriwaki, and T. Shimizu, *Jpn. J. Appl. Phys.* **34**, L174 (1995).
[4] K. Hayasaka, *Opt. Commun.* **206**, 401 (2002).
[5] K. Matsubara, S. Uetake, H. Ito, Y. Li, K. Hayasaka, and M. Hosokawa, *Jpn. J. Appl. Phys.* **44**, 229 (2005).
[6] R. Blümel, C. Kappler, W. Quint, and H. Walther, *Phys. Rev. A* **40**, 808 (1989).